Petroleum Research 2 (2017) 178–185

Contents lists available at ScienceDirect

Petroleum Research

journal homepage: http://www.keaipublishing.com/en/journals/petroleum-research/

A new measurement method for radial permeability and porosity of shale

Zehao Yang [a, b], Mingzhe Dong [a, *]

[a] Department of Chemical and Petroleum Engineering, University of Calgary, Calgary AB T2N 1N4, Canada
[b] School of Petroleum Engineering, China University of Petroleum, Shandong 266580, China

ARTICLE INFO

Article history:
Received 5 September 2016
Received in revised form
22 December 2016
Accepted 28 December 2016

Keywords:
Radial permeability and porosity
Pressure attenuation
Annular space
Concentration conductivity coefficient
Shale

ABSTRACT

To more conveniently and accurately obtain the radial permeability of shale, a new measurement method was proposed for the pressure attenuation of radial permeability and porosity in shale. Through experiments, this method could be used to get the pressure attenuation curve in annular space between the core and inner wall of PVT vessel under the helium along shale radial flow. Accordingly, a mathematical model was established to obtain the semi-analytical solution between pressure and time in the radial model. Meanwhile, through fitting the experimental results, the concentration conductivity and porosity of shale were obtained, and their relationship was used to derive the radial permeability of shale. This method was adopted to measure the permeability and porosity of two cores under three sets of different initial pressures in the annular space. The permeability test results were compared with those obtained by the conventional Dicker method and Smits pressure-attenuation method, and the porosity test results were also compared with those obtained by the conventional porosimeter, thus the feasibility and superiority of this method were confirmed. In contrast to the conventional pressure-attenuation methods, this new model had advantages of simpler instruments and more convenient operation, and was also easy to measure the radial permeability and porosity of shale.

1. Introduction

With development of economy, the unconventional oil and gas, particularly shale gas, had been paid more and more wide attention (Guo and Wang, 2013; Zhang and Yang, 2013). The most important characteristic of shale was the ultralow permeability, which was one of difficulties in shale gas exploration. In order to better guide the shale gas exploration, it was important to accurately measure shale permeability. The method of the pressure attenuation in core axial direction was often adopted for routine measurement of shale permeability, but diffusion flows of shale gas occurred in three-dimensional directions simultaneously. Thus, how to obtain the radial permeability was of great importance to researches on the seepage laws and exploration schemes of shale gas.

Brace et al. (1968) first put forward the pressure-attenuation experiment method, and measured the permeability of tight core using the mathematical model. It was assumed that the pressure gradient was a constant in the process of gas flow, and a semi-analytical solution of the mathematical model was determined. In this model, the pressure was proportional to the semi-logarithm of time, and the permeability was obtained by use of slope. However, this model was only applicable to the low-porosity core. According to the Brace's theory, the numerical fitting was conducted on the stress and time curve by Lin (1977) to obtain the permeability of tight cores. The analytical solution of the Brace attenuation model was given by Hsieh et al. (1981), so as to more accurately calculate the permeability of shale. However, due to the complexity of analytical results, this model was also not widely applied. According to the numerical solution method of Lin, Bourbie and Walls (1982) discovered that the numerical solution had a greater error compared with the given semi-analytical solution, and thus redesigned the mathematical model of Brace, but the given calculation process of model solution was still very complicated. Through modification of the model of Heieh, Dicker and Smits (1988) put forward the current widely-used pressure-attenuation method for measuring the permeability of tight cores; this method aimed to achieve faster and more accurate solution by the proper porosity volume ratio of the gas upstream and downstream in the

* Corresponding author.
E-mail address: mtdong@ucalgary.ca (M. Dong).
Peer review under responsibility of Petroleum Research.

http://dx.doi.org/10.1016/j.ptlrs.2017.07.004

attenuation experiments. On this basis, the pressure-attenuation method was developed and had became the most major measurement method for the permeability of tight cores, and it was extensively used (Haskett et al., 1988; Jones, 1997; Zhang et al., 2000a, 2000b; Liang et al., 2001; Li et al., 2004; Comisky et al., 2007; Fedor et al., 2008; Cui et al., 2009; Sarker et al., 2009; Civan et al., 2011; Guo et al., 2013; Xue and Ehlig-Economides, 2013; Yang et al., 2015).

Since the pressure-attenuation method was proposed, the measurement methods of tight core permeability were mostly established on the basis of the Brace model; as a one-dimensional axial model, the Brace model could only be used to measure the core axial permeability; meanwhile, only through coring on the radial plane, the shale radial permeability then could be measured using the Dicker and Smits method. For this problem, the authors proposed a new idea for measuring permeability so as to solve the radial permeability: (1) The traditional pressure-attenuation method needed to obtain the pressure difference between the upper and lower end face, so it was unable to directly measure the radial permeability of cores; but using the authors' method, it was only required to obtain the pressure change-time relation curve at the entry end. (2) According to the Brace model, it was required to measure the porosity firstly and permeability secondly of tight cores (Jones, 1997), while the authors' method was able to solve the permeability and obtain the core porosity simultaneously. (3)The instruments in the authors' method were simple, the experimental operation was more convenient, and only a precise pressure sensor was needed in the experiment; while the Brace model required more precise pressure sensors.

2. Experiment

2.1. Experimental instruments

To measure the radial permeability of shale, it was required to ensure the gas radial flow along the core, and therefore the PVT container was redesigned for the experiment (Fig. 1). Two cores from the Fuling area in Chongqing were used in the experiment, the diameter and length of the core was 2.54 cm and 3.26 cm respectively, and the upper and lower end of the core were sealed wit the epoxy resin to prevent gas inflow from the axial direction. The core was placed into the center of the PVT container with the inner diameter of 3.6 cm, and its upper and lower end faces were fixed by the clamping device to guarantee the horizontal placement of the core. The whole experimental system device was shown in Fig. 2; the PVT container provided the place for the gas radial flow; the intermediate container was used to store gas, and connected with the PVT container. Meanwhile, the hand pump was used to adjust position of the piston in the intermediate container, thus to adjust and control the initial pressure of gas in the PVT container. The water bath system was used to keep the system temperature constant. Moreover, the pressure sensor was applied to record the pressure change in the PVT container, and the pressure sensor range was from 0 to 20.7 MPa (0–3000 psi), the pressure accuracy was 3.45 kPa (0.5 psi) and could be estimated to 0.345 kPa (0.05 psi), the changed pressures were collected by the computer.

2.2. Experiment process

The experimental process was shown as below. Firstly, the pressured 10 MPa helium was transported to the device for sealing test, after one day of the pressure leak test, the pressure change was less than 2 kPa. Secondly, after drying in oven for 3 d, shale cores were taken out and both ends of the cores were sealed by the epoxy resin. Third, the core was placed in the center of the PVT container, and the upper and lower end faces of the cores were contacted with the clamping device completely, and the cores were fixed through the clamping device. Fourth, the whole system was placed in the constant temperature water bath, and then was vacuumed after the temperature was kept at a constant. Fifth, the valve was opened to enable the intermediate container connecting with the PVT container; the hand pump was used to adjust the gas pressure until the pressure reached the initially set pressure, and the equilibrium time was about 2 h; here, the fluid pressure in the shale pore was the initial pressure (p_i), and the purpose of setting the certain initial pressure was to remove effects of gas slippage effect (Dong et al., 2012). Sixth, the oil pressure pump was adopted to add the axial confining pressure (p_c) to the clamping device, and the confining pressure was higher than the initial fluid pressure in pores by 3 MPa, and thus the clamping device and core end face were completely sealed. Seventh, the valve between the intermediate container and the PVT container was closed, and then the hand pump was used to increase pressure by 2 MPa in the intermediate container; afterwards, the valve between the intermediate container and the PVT container was opened, so the gas pressure in the annular space would rise quickly, until the pressure value in the annular space increased by about 1.5 MPa, then the valve was closed immediately, and the pressure values were recorded after reaching pressure equilibrium in the annular space of the PVT container; at that time, the pressure in the annular space of the PVT container was slightly higher than the fluid pressure in shale pores. It was especially worth noting that according to the calculation model, when the pressure changed little, the high pressure physical property of the helium gas could be considered as the constant which was equal to values under the average pressure of the annular pressure and the fluid pressure, so that the increase of pressure in the annular space of the PVT container would better not exceed 2 MPa.

2.3. Initial pressure conditions

Through the experiment, the initial fluid pressures of the annular space and shale pores were obtained in the radial permeability measurement of two cores from Fuling, Chongqing (Table 1).

From Table 1, the fluid pressures could be accurately controlled by the hand pump, while the annular pressure was controlled by the manual controlling valve, so the initial pressure difference was

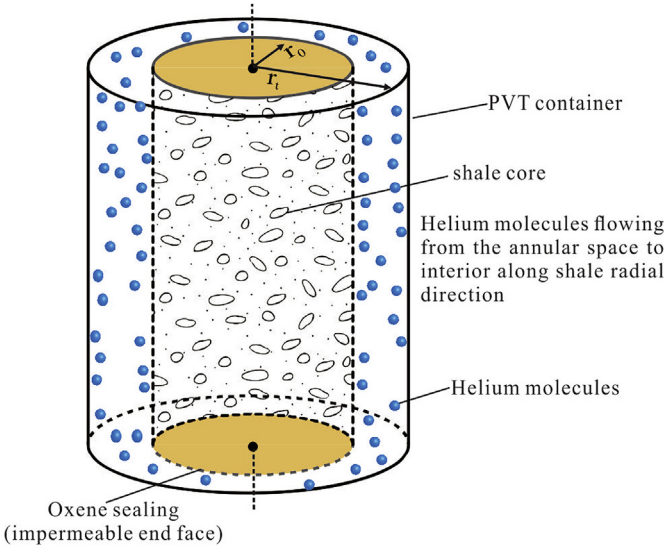

Fig. 1. Schematic diagram of helium flow along the radial direction. r_0 was the core sample radius, m; r_t was the inner diameter of the PVT container, m.

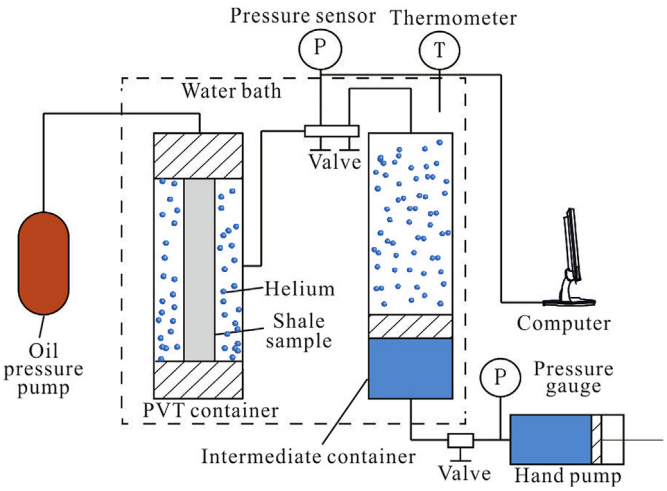

Fig. 2. Experimental device.

about 1.5 MPa, but this would not cause inaccurate measurement, because only the pressure change data of the annular space were used for data analysis, under the gas sealing condition, the pressure sensor could accurately measure such a change. Meanwhile, the previous experiment had illustrated that the confining pressure was 3 MPa higher than the initial fluid pressure.

3. Relationship between concentration conductivity and permeability

In this study, as the method for solving the permeability was established based on the concentration conductivity of gas in porous media, it was required to define the concept of the concentration conductivity and its relationship with permeability.

In the chemical field, the diffusion coefficient was commonly used to describe the molecular diffusion effect caused by molecular concentration difference in the liquid, and the focus was put on the intermolecular effect. However, rocks were the porous media, so besides the effect between gas molecules during gas flow in pores, the molecular collisions with pore wall could not be ignored. Therefore, the concept of the concentration conductivity was adopted herein to describe the gas flow process in the porous medium (Cui et al., 2009). The relationship between the concentration conductivity and the permeability could be illustrated by the physical model in Fig. 3. Fig. 3 showed the steady gas flow in the one-dimensional core, the gas concentration at the inlet and outlet was kept as c_1 and c_2, respectively, and the former was slightly greater than the latter. Because of the constant mass flow of gas flowing through the section, the following could be obtained.

$$J_0 = \frac{\rho_0 Q_0}{MA} \tag{1}$$

where J_0 was the molar flux for shale arbitrary cross section, mol/(m^2 s); ρ_0 was the helium density under the pressure of p_0, kg/m^3; Q_0 was the helium flow in a cross section, m^3/s; M was the molar mass of helium, kg/mol; A was the cross-sectional area of the core, m^2.

According to Fick's Law (Hao et al., 1994), it could also be expressed as below.

$$J_0 = -\kappa \frac{dc}{dx} \tag{2}$$

where κ was the concentration conductivity after expansion, m^2/s; c was the concentration, mol/m^3.

In the porous media, the gas flow was caused by the existence of the concentration gradient (or the pressure gradient), so that it could be considered that the gas flow flux was jointly determined by the concentration gradient and the concentration conductivity. Equation (2) was substituted into Equation (1) to obtain Equation (3) as below:

$$\kappa = \frac{\rho_0 Q_0 L}{MA(c_1 - c_2)} \tag{3}$$

where c_1 was the molar concentration of helium at the inlet end, mol/m^3; c_2 was the molar concentration of the helium at the outlet end, mol/m^3; L was the core length, m.

According to the real gas state equation, the followings could be obtained:

$$c_1 - c_2 = \Delta c = \frac{\Delta p}{\bar{z}RT} \tag{4}$$

$$\rho_0 = \frac{p_0 M}{z_0 RT} \tag{5}$$

where z_0 was the gas compressibility factor under the pressure of p_0; $\bar{z}$ was the average compressibility factor of inlet and outlet ends (the average value was used herein due to the above hypothesis that Δc was small, and thus the compressibility factor changed largely); p_0 was the pressure of core at a cross section, Pa; R was the ideal gas constant which was equal to 8.314 J/(mol K); T was the temperature, K; Δc was the gas concentration difference between the inlet end and the outlet end, mol/m^3; Δp was the pressure difference between the inlet end and the outlet end, Pa.

Equations (4) and (5) were substituted into Equation (3) to obtain the expression of concentration conductivity:

$$\kappa = \frac{\frac{p_0 M}{z_0 RT} Q_0 L}{MA\frac{\Delta p}{\bar{z}RT}} = \frac{\bar{z} p_0 Q_0 L}{z_0 A \Delta p} = \frac{\bar{p}\bar{Q}L}{A\Delta p} \tag{6}$$

where $\bar{p}$ was the average pressure of the inlet end and the outlet end, Pa, $\bar{p} = (p_1 + p_2)$; $\bar{Q}$ was the average flow of the inlet end and the outlet end, m^3/s, $\bar{Q} = (Q_1 + Q_2)/2$; $\bar{\rho}$ was the average density of the inlet end and the outlet end, kg/m^3.

Equation (6) was transformed to obtain the average flow at the

Table 1
Initial pressures in the experiment.

Group	Sample 1		Sample 2	
	Annular pressure /MPa	Flow pressure /MPa	Annular pressure /MPa	Flow pressure /MPa
1	6.54	5	6.53	5
2	9.54	8	8.52	8
3	11.54	10	11.53	10

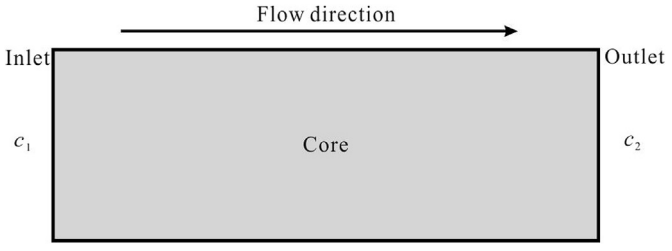

Fig. 3. Gas flow along the core sample.

inlet end and the outlet end:

$$\overline{Q} = \frac{\kappa A \Delta p}{\overline{p} L} \tag{7}$$

Fluids flowed in the porous medium, and the following could be obtained according to the Darcy Law:

$$Q = -\frac{KA}{\mu}\frac{\mathrm{d}p}{\mathrm{d}x} \tag{8}$$

where K was the core permeability, D; μ was the helium viscosity, Pa s.

Due to the constant mass flow on each section, according to Boyle-Mariotte Law under the isothermal conditions, changes of gas volume flow with pressure could be expressed as below.

$$Q = \frac{p_0 Q_0}{z_0}\frac{z}{p} \tag{9}$$

where z was the gas compressibility factor; p was the pressure, MPa.

When the pressure difference between inlet and outlet ends was not large, the average pressure of the inlet end and the outlet end could be used to represent the physical properties of gas. Equation (8) was united with Equation (9) to obtain the followings:

$$\overline{Q} = \frac{p_0 Q_0}{z_0}\frac{\overline{z}}{\overline{p}} = \frac{KA}{\overline{\mu}}\frac{\Delta p}{L} \tag{10}$$

where $\overline{\mu}$ was the average viscosity of the inlet end and the outlet end, Pa s.

Equation (10) was substituted into Equation (7) to obtain the relationship between permeability and concentration conductivity as below:

$$\kappa = \frac{K\overline{p}}{\overline{\mu}} \tag{11}$$

According to the real gas state equation, the following could be obtained:

$$\overline{p} = \frac{\overline{z}\overline{\rho}RT}{M} \tag{12}$$

Equation (12) was substituted into Equation (11) to obtain the expression as below:

$$\kappa = \frac{K\overline{z}\overline{\rho}RT}{M\overline{\mu}} \tag{13}$$

Because k was the concentration conductivity at a cross section, whereas the concentration conductivity in the pores was expressed as below:

$$\kappa_\phi = \frac{\kappa}{\phi} = \frac{K\overline{z}\overline{\rho}RT}{M\overline{\mu}\phi} \tag{14}$$

where ϕ was the core porosity; k_ϕ was the concentration diffusion coefficient of rock pores, m^2/s.

Equation (14) could also be expressed as below:

$$K = \frac{\kappa_\phi M\overline{\mu}\phi}{\overline{z}\overline{\rho}RT} \tag{15}$$

When the length of the core model was infinitesimal, Equation (15) could express the relationship between the core permeability and the concentration conductivity at any point:

$$K = \frac{\kappa_\phi M\mu\phi}{z\rho RT} \tag{16}$$

From Equation (16), the concentration conductivity was not only related with the permeability, but also correlated to the nature of gas. Therefore, based on the concentration conductivity, the mathematical model could be established to calculate the porosity and permeability of shale core.

4. Theoretical model

4.1. Hypothesis of the model

In this study, the mathematical model was established based on experiments, and some reasonable simplified hypotheses had been made for the actual situation as below: (1) the concentration conductivity in pores was a constant; (2) the gas only flowed in the radial direction without inflowing from two end faces; (3) no adsorption phenomenon occurred in the helium gas; (4) a constant temperature was kept in the whole experiment process; (5) the slippage effect was ignored; (6) the concentration of shale inlet end was always remained as the equilibrium concentration under the PVT container pressure, here the equilibrium concentration was the concentration at which the gas eventually reached equilibrium in PVT the container during the experiment.

To verify reliability of the model simplification, each hypothesis was discussed as below. In the hypothesis (1) was that the gas concentration conductivity in pores was a constant, and the premise was that values of gas attenuation relative to testing pressure were very small. For example, the test pressure in the annular space of the PVT container was above 6.5 MPa, while the values of pressure attenuation was only 10–100 kPa, and then the concentration conductivity was considered as a constant in the radial model. As shown in Fig. 4, within range of testing pressure, the concentration conductivity corresponding to cores with different permeability changed very slowly with pressure, while the changed pressure was relatively small, the concentration conductivity could be regarded as a constant. In the hypothesis (2), the gas could not flow along axial direction, this was because that not only both ends of the experimental core were sealed by the epoxy resin, but also the axial pressure was imposed between the clamping device and the core end face, therefore, the gas could not inflow from both end faces, but just only inflow along radial direction of cores. In the hypothesis (3), the helium was the single-phase flow, this was because that the system was vacuumed before the experiment and then completely filled with the helium. In the hypothesis (4), due to the experiment beginning after the temperature test, the influence of the temperature fluctuation on pressure could be ignored. In the hypothesis (5), the shale was saturated by gas with a certain pressure, the slippage effect could be ignored (Dong et al., 2012), and this hypothesis was also used in the traditional pressure-attenuation methods (Haskett et al., 1988; Jones, 1997; Zhang et al., 2000a, 2000b; Liang et al., 2001; Li et al., 2004; Comisky et al., 2007; Fedor et al., 2008; Cui et al., 2009; Sarker et al., 2009; Civan et al., 2011; Guo et al., 2013; Xue and Ehlig-Economides, 2013). In the hypothesis (6), the gas concentration at the inlet end could be remained as the equilibrium concentration, the premise was that values of gas attenuation in the PVT container relative to testing pressure were very small; this hypothesis had been verified in the chemical industry and often was applied in the determination of diffusion coefficient (Zhang et al., 2000c; Etminan et al., 2013; Behzadfar and Hatzikiriakos, 2014; Etminan et al., 2014; Kavousi et al., 2014).

4.2. Model establishment and solution

Due to the concentration gradient between the shale inlet end and the PVT container, the gas molecules could flow along the shale radial direction, and the concentration in the PVT container would be decreased accordingly. The mass conservation could be used to establish the model as below:

$$\frac{\partial c}{\partial t}=\frac{1}{r}\frac{\partial}{\partial r}\left(r\kappa_{\phi}\frac{\partial c}{\partial r}\right) \tag{17}$$

The boundary conditions were shown as following:

$$c|_{t>0,r=r_0}=c_{\mathrm{eq}} \tag{18}$$

$$\left.\frac{\partial c}{\partial r}\right|_{t>0,r=0}=0 \tag{19}$$

where t was the time, s; r was the radius, m; r_0 was the radius of the tested core, m; c_{eq} was the eventual equilibrium concentration of the PVT container, umol/m^3. c_{eq} was the function of the temperature and the equilibrium pressure, and because the experiment was operated in an isothermal process, so it was only related to the equilibrium pressure.

The initial conditions were shown as below:

$$c|_{t=0,0\le r<r_0}=c_{\mathrm{i}} \tag{20}$$

where c_{i} was the initial concentration of shale, mol/m^3.

Through the Laplace transformation of the above mathematical model, the distribution function of helium in the radial direction of shale was obtained (Crank, 1975):

$$\frac{c-c_{\mathrm{i}}}{c_{\mathrm{eq}}-c_{\mathrm{i}}}=1-\frac{2}{r_0}=\sum_{n=1}^{\infty}\frac{\mathrm{e}^{-\kappa_{\phi}\mathrm{a}_n^2 t}J_0(ra_n)}{\mathrm{a}_n J_1(r_0 a_n)} \tag{21}$$

where a_{n} was the positive root of $J_0(r_0 a_{\mathrm{n}})$ of the zero-order Bessel function.

According to the real gas state equation, the following could be obtained:

$$pV=znRT \tag{22}$$

where V was the volume between the core and the cylindrical PVT container, $V=\pi(\mathrm{r}^2_{\mathrm{t}}\text{-}\mathrm{r}^2_0)l$, m^3; l was the length of the core, m; n was the substance amount in the annular space, mol; r_{t} was the inner diameter of the PVT container, m.

Because the reduced helium substance amount per unit time in the annular space of PVT container was equal to the substance amount through the shale radial end face per unit time, the following equation could be obtained:

$$\frac{\mathrm{d}n}{\mathrm{d}t}=\frac{V}{zRT}\frac{\mathrm{d}p}{\mathrm{d}t}=-\kappa_{\phi}\phi A\left.\frac{\partial c}{\partial r}\right|_{r=r_0} \tag{23}$$

where A was the area of the lateral surface of the cylindrical core, $A=2\pi r_0 l$, m^2.

Because the r was equal to the r_0, then

$$\left.\frac{\partial c}{\partial r}\right|_{r=r_0}=(c_{\mathrm{eq}}-c_i)\sum_{n=1}^{\infty}\frac{2}{r_0}\mathrm{e}^{-\kappa_{\phi}a_n^2 t} \tag{24}$$

Equation (24) was substituted into Equation (23), and then the infinite processing was conducted on time integral (i.e., equilibrium moment) to obtain the change law of pressure with time as follows:

$$p(t)=\frac{2A\phi\left(p_{\mathrm{eq}}-p_{\mathrm{i}}\right)}{r_0 V}\sum_{n=1}^{\infty}\frac{e^{-\kappa_{\phi}a_n^2 t}}{a_n^2}+p_{\mathrm{eq}} \tag{25}$$

where P_{eq} was the equilibrium pressure, Pa; P_{i} was the initial saturated pressure in pores, Pa.

Due to rapid convergence in Equation (25), the first term could be simplified as below:

$$p(t)=\xi e^{-\gamma t}+p_{\mathrm{eq}} \tag{26}$$

In Equation (26), $\xi=\frac{4\phi(p_{\mathrm{eq}}-p_{\mathrm{i}})}{a_1^2(r_{\mathrm{t}}^2-r_0^2)}$, $\gamma=\kappa_{\phi}a_1^2$; a_1 was the minimal positive root of a_{n}.

Through the experimental data, the simple fitting was conducted on Equation (26) to calculate the concentration conductivity, the equilibrium pressure and the porosity. Moreover, the relationship between concentration conductivity and permeability could be used to acquire the radial permeability of the core.

5. Solution of core parameter

According to the given experimental method in this paper, three groups of experiments were carried out on two cores collected from Fuling area in Chongqing under the condition of different pressures respectively, and the experimental and fitting results were shown in Fig. 5.

Group 1 experimental result of Sample 1 was used to illustrate the use of this model. At the beginning of the experiment, the shale was saturated by helium, the pressure was 5 MPa, while the pressure in the annular space between the PVT container and the shale sample was 6.52 MPa; in the meantime, the gas in the annular space could flow into the shale soon. It should be noted that within a short time at the beginning, the pressure value was invalid, this was because that the gas was unable to pass through the whole shale in the radial direction, the permeability measured in this period was not the average shale radial permeability, and it changed with the length of the core. The duration of this period was determined by the fitting degree of experimental data in this model.

First, a_1 in Equation (26) was solved. Assuming that z_1 was the first positive root of the zero-order Bessel equation $j_0(z)=0$, then z_1 was equal to 2.405, thus $a_1=z_1/r_0=2.405/r_0$. It could be seen that a_1 was decided by the radius of the core. The relationship between a_1 and the core radius was shown in Fig. 6, because the core radius was 1.27 cm in this experiment, the corresponding a_1 was 189 m^{-1}.

The Group 1 experimental data were fitted in accordance with Equation (26), then ξ was equal to 38.40 kPa, γ was equal to 0.0085, and the equilibrium pressure (P_{aq}) was equal to 6464.7 kPa. Then the followings were obtained:

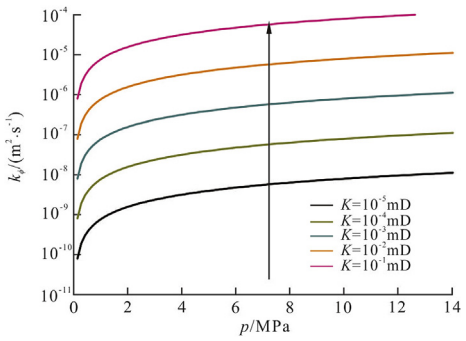

Fig. 4. Relationship between pressure and concentration conductivity under different permeabilities.

$$\phi = \frac{a_1^2\left(r_t^2 - r_0^2\right)\xi}{4\left(p_{eq} - p_i\right)} = \frac{189^2 \times \left(0.018^2 - 0.0127^2\right) \times 38.40}{4 \times (6464.7 - 5000)} = 0.038 \quad (27)$$

$$\kappa_\phi = \frac{\gamma}{a_1^2} = \frac{0.0085}{189^2} = 2.38 \times 10^{-7}\mathrm{m}^2/\mathrm{s} \quad (28)$$

Equations (27) and (28) were used to calculate the shale porosity which was 3.8%, and the concentration conductivity of helium in pore was 2.38×10^{-7} m^2/s.

The helium compressibility factor and viscosity met with the rule shown in Fig. 7 (Stroud et al., 1960; Lee et al., 1966; Gracki et al., 1969; McCarty, 1973). Moreover, it could also be seen in Fig. 7 (b) that when the helium pressure was not very high (generally within 25 MPa), the viscosity was only the function of the temperature.

Because the Group 1 experimental temperature was 30 °C, the initial average pressures of the shale pore and the PVT container all were 5.76 MPa, so the helium viscosity (μ) was equal to 0.021 mP s and the compressibility factor (z) was equal to 1.025, the real gas state equation could be applied to obtain density of the helium as below:

$$\rho = \frac{PM}{ZRT} = \frac{5.76 \times 10^6 \times 0.004}{1.025 \times 8.314 \times (30 + 273.15)} = 8.92\mathrm{kg/m}^3 \quad (29)$$

The above parameters were substituted to Equation (16), and the radial permeability of the shale in the Group 1 experiment was showed as follows:

$$K = \frac{\kappa_\phi M \mu \phi}{z\rho RT} = \frac{2.38 \times 10^{-7} \times 0.004 \times 0.000021 \times 3.8\%}{1.025 \times 8.92 \times 8.314 \times 303.15} = 3.30 \times 10^{-5}\mathrm{mD} \quad (30)$$

According to other five groups of experimental results, porosities and permeabilities of two shale samples could be obtained as shown in Table 2.

Through a comparison between the initial pressure of Table 1 and the result of Table 2, it could be seen that with increase of the initial saturation pressure of shale, permeabilities of two shale core samples gradually increased, and porosities also increased

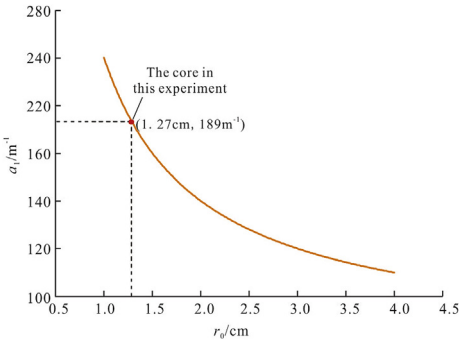

Fig. 6. Relationship between the core radius (r_0) and the coefficient (a_1).

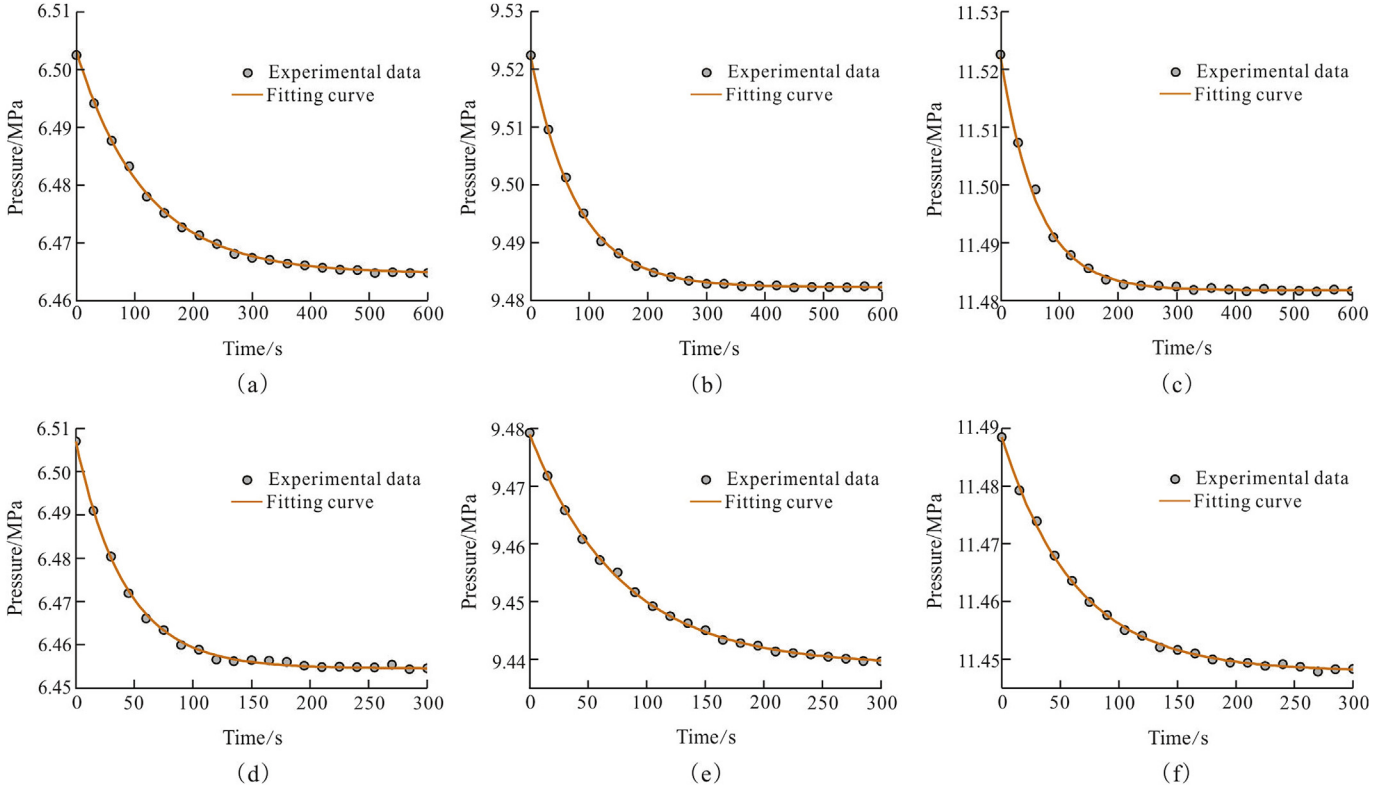

Fig. 5. Fitting curves of gas pressure and time in the annular space between the PVT container inner wall and the core external wall under different initial pressures. (a) The initial pressure in the annual space of Sample 1 at 6.52 MPa; (b) the initial pressure in the annual space of Sample 1 at 9.54 MPa; (c) the initial pressure in the annual space of Sample 1 at 11.54 MPa; (d) the initial pressure in the annual space of Sample 2 at 6.53 MPa; (e) the initial pressure in the annual space of Sample 2 at 9.52 MPa; (f) the initial pressure in the annual space of Sample 2 at 11.53 MPa.

accordingly. This was because that the sensitivity of shale in the region to fluid pressure changes was greater than that to the confining pressure changes (Ghabezloo et al., 2009), i.e., under the same net confining pressure, with the increase of fluid pressure, the permeability would increase accordingly as cores were more sensitive to fluid pressure.

6. Discussion

The models for the permeability measurement of tight cores through of the pressure-attenuation method were mostly developed from the Brace model; the most common method was the Dicker and Smits' model, and its experimental device was shown in Fig. 8 (Dicker and Smits, 1988). This method required multiple precise pressure gauges, and meanwhile, the core porosity was acquired ahead in this model. Moreover, this method was also required to improve the measurement precision by controlling the upstream and downstream volume ratios, so that the control process of experiment system was complex. To improve the accuracy of this method in the study, the same-size pieces were drilled on the radial plane of two shale samples during drilling experiment cores (samples 1 and 2), respectively, and the permeability measurement instrument designed from the Dicker and Smits' method was used to perform three groups of experiments on two cores (samples 3 and 4) under the same pressure condition in the above method, and to measure the axial permeability. In the experimental results, the axial permeabilities of sample 3 was 0.332×10^{-6} mD, 0.339×10^{-6} mD and 0.346×10^{-6} mD, respectively, and those of Sample 4 were 0.0127×10^{-6} mD, 0.0138×10^{-6} mD and 0.0146×10^{-6} mD, respectively. Through comparison of the core permeability values (Table 2) measured using the above method, it could be seen that the results were all on the same order of magnitude, while the major reason for different results only was the heterogeneity affects of shale; to some extent, this comparison also proved the accuracy of the method. Meanwhile, the conventional porosity measurement instrument designed by the static capacity method was applied to measure the porosity of Samples 3 and 4. The measurement porosities of Samples 3 and 4 were 3.84% and 5.54%, respectively, as compared with the porosity results from the above method, the error was within 5%.

In order to make the measurement results more accurate and stable, four aspects to control the experimental error should be noted.

(1) The temperature control. The whole experiment system must be placed in the water bath or constant temperature oven to keep a constant temperature in the experiment, this was because under condition of small annular space, change of temperature had a larger effect on change of gas pressure.
(2) Control of net confining pressure. In the experiment, the net confining pressure of each group should be set similarly, this was because that the core had the pressure-sensitive effect, only when the confining pressure was close to the average fluid pressure (the average value of the annular pressure and the fluid pressure), permeabilities measured in the experiment were of the correlation significance.
(3) Control of slippage effect. In order to minimize the slippage effect on the measurement results, the pressure difference between the annular pressure and the flow pressure should be less than 2 MPa (Dong et al., 2012).
(4) Control of gas sealing. Seal inspections were required prior to the experiment, because the system gas leakage had great influences on measurement results.

Table 2
Permeability and porosity of shale samples through experiments.

Group	Sample 1		Sample 2	
	Permeability /mD	Porosity /%	Permeability /mD	Porosity /%
1	3.30×10^{-5}	3.80	1.27×10^{-5}	5.23
2	3.38×10^{-5}	3.92	1.38×10^{-5}	5.68
3	3.46×10^{-5}	3.98	1.46×10^{-5}	2.72

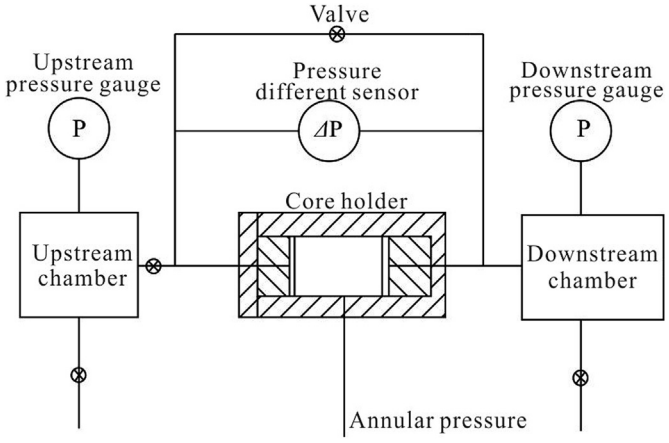

Fig. 8. The Dicker and Smits' experimental device.

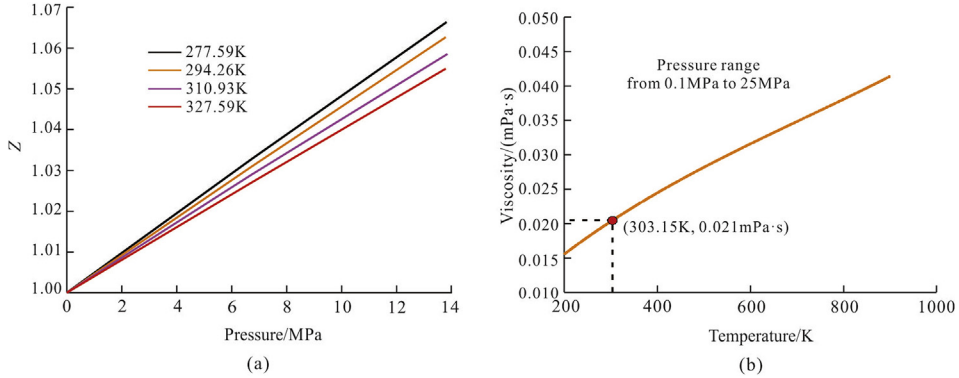

Fig. 7. Physical properties of helium. (a) Relationship between the compressibility factor and pressure as well as temperature; (b) relationship between temperature and viscosity.

7. Conclusions

(1) Two shale core samples were used to carry out three groups of experiment. Although the initial pressure of the PVT container in each group was not the same, the errors of the final measured permeability were within 5%, indicating the experimental method had a good stability.
(2) Compared the measured permeabilities through the method in this study with those obtained by the traditional Dicker and Smits' method, within the allowable range of the experimental error, the measured values of these two methods were consistent; compared the measured porosities through the method in this study with those obtained by the conventional porosity measurement instrument, the test results of these two methods were also consistent. That indicated the experiment method had a good accuracy.
(3) Due to simple experimental device and convenient experimental operation, only the pressure in the annular space in the experiment should be measured, and the upstream and downstream pressured needed not be measured, therefore, less pressure measuring devices were needed, leading to more concise experimental operation.
(4) Sensitivity of the core on fluid pressure was greater than sensitivity of the cores on the confining pressure, therefore, with the increase of the initial pressures, the measured core permeability would increase.

Acknowledgements

This work was supported by National Key Basic Research Program of China (973 Program) (No. 2014CB239103), Natural Sciences and Engineering Research Council of Canada (NSERC) – Canada Excellence Research Chair (CERC) and China University of Petroleum (East China) Postgraduate Innovation Project (No. YCX2017018).

References

Behzadfar, E., Hatzikiriakos, S.G., 2014. Diffusivity of CO_2 in bitumen: pressure–decay measurements coupled with rheometry. Energy & Fuels 28 (2), 1304–1311.
Bourbie, T., Walls, J., 1982. Pulse decay permeability: analytical solution and experimental test. Soc. Pet. Eng. J. 22 (5), 719–721.
Brace, W.F., Walsh, J.B., Frangos, W.T., 1968. Permeability of granite under high pressure. J. Geophys. Res. 73 (6), 2225–2236.
Civan, F., Rai, C.S., Sondergeld, C.H., 2011. Shale Permeability Determined by Simultaneous Analysis of Multiple Pressure-pulse Measurements Obtained under Different Conditions: North American Unconventional Gas Conference and Exhibition. Society of Petroleum Engineers, Texas.
Comisky, J.T., Newsham, K., Rushing, J.A., Blasingame, T., 2007. A Comparative Study of Capillary-pressure-based Empirical Models for Estimating Absolute Permeability in Tight Gas Sands. Society of Petroleum Engineers, Anaheim.
Crank, J., 1975. The Mathematics of Diffusion. Clarendon Press, Oxford.
Cui, X., Bustin, A.M.M., Bustin, R.M., 2009. Measurements of gas permeability and diffusivity of tight reservoir rocks: different approaches and their applications. Geofluids 9 (3), 208–223.
Dicker, A.I., Smits, R.M., 1988. A Practical Approach for Determining Permeability from Laboratory Pressure-pulse Decay Measurements. Society of Petroleum Engineers, Richardson.
Dong, M., Li, Z., Li, S., Yao, J., 2012. Permeabilities of tight reservoir cores determined for gaseous and liquid CO_2 and C_2H_6 using minimum backpressure method. J. Nat. Gas Sci. Eng. 5, 1–5.
Etminan, S., Pooladi-Darvish, M., Maini, B.B., Chen, Z., 2013. Modeling the interface resistance in low soluble gaseous solvents-heavy oil systems. Fuel 105, 672–687.
Etminan, S.R., Maini, B.B., Chen, Z., 2014. Determination of mass transfer parameters in solvent-based oil recovery techniques using a non-equilibrium boundary condition at the interface. Fuel 120, 218–232.
Fedor, F., Hámos, G., Jobbik, A., Máthé, Z., Somodi, G., 2008. Laboratory pressure pulse decay permeability measurement of Boda claystone, Mecsek Mts., SW Hungary. Phys. Chem. Earth, Parts A/B/C 33, S45–S53.
Ghabezloo, S., Sulem, J., Guédon, S., Martineau, F., 2009. Effective stress law for the permeability of a limestone. Int. J. Rock Mech. Min. Sci. 46 (2), 297–306.
Gracki, J.A., Flynn, G.P., Ross, J., 1969. Viscosity of nitrogen, helium, hydrogen, and argon from −100 to 25°C up to 150–250 atmosphere. J. Chem. Phys. 51 (9), 3856–3863.
Guo, C., Bai, B., Wei, M., He, X., Univeristy, M., 2013. Study on Gas Permeability in Nano Pores of Shale Gas Reservoirs. Society of Petroleum Engineers, Calgary.
Guo, S.B., Wang, Y.G., 2013. Shale gas accumulation conditions and exploration potential of carboniferous benxi formation in ordos basin. Acta Pet. Sin. 34 (3), 445–452 (in Chinese).
Hao, S.S., Huang, Z.L., Yang, J.Y., 1994. Dynamic Balance of Natural Gas Migration and Accumulation and its Application. Petroleum Industry Press, Beijing, pp. 3–55 (in Chinese).
Haskett, S.E., Narahara, G.M., Holditch, S.A., 1988. A method for simultaneous determination of permeability and porosity in low-permeability cores. SPE Form. Eval. 3 (3), 651–658.
Hsieh, P.A., Tracy, J.V., Neuzil, C.E., Bredehoeft, J.D., Silliman, S.E., 1981. A transient laboratory method for determining the hydraulic properties of 'tight' rocks—I. Theory. Int. J. Rock Mech. Min. Sci. Geomech. Abstr. 18 (3), 245–252.
Jones, S.C., 1997. A technique for faster pulse-decay permeability measurements in tight rocks. SPE Form. Eval. 12 (1), 19–25.
Kavousi, A., Torabi, F., Chan, C.W., Shirif, E., 2014. Experimental measurement and parametric study of CO_2 solubility and molecular diffusivity in heavy crude oil systems. Fluid Phase Equilib. 371, 57–66.
Lee, A.L., Gonzalez, M.H., Eakin, B.E., 1966. Viscosity of methane/n-decane mixtures. J. Chem. Eng. Data 11 (3), 281–287.
Li, S., Dong, M., Dai, L., Li, Z., Pan, X., 2004. Determination of Gas Permeability of Tight Reservoir Cores without Using Klinkenberg Correlation. Society of Petroleum Engineers, Perth.
Liang, Y., Price, J.D., Wark, D.A., Watson, E.B., 2001. Nonlinear pressure diffusion in a porous medium: approximate solutions with applications to permeability measurements using transient pulse decay method. J. Geophys. Res. Solid Earth 106 (B1), 529–535.
Lin, W., 1977. Compressible Fluid Flow through Rocks of Variable Permeability. Lawrence Livermore Lab, Livermore.
McCarty, R.D., 1973. Thermodynamic properties of helium 4 from 2 to 1500 K at pressures to 108 Pa. J. Phys. Chem. Ref. Data 2 (4), 923–1042.
Sarker, R., Batzle, M., Lu, N., 2009. Determination of Fluid Permeability and Specific Storage in Tight Rocks from 1-D Diffusion Induced by Constant Rate Fluid Injection. Society of Exploration Geophysicists, Houston.
Stroud, L., Miller, J.E., Brandt, L.W., 1960. Compressibility of helium at -10° to 130° F. and pressures to 4000 P.S.I.A. J. Chem. Eng. Data 5 (1), 51–52.
Xue, H., Ehlig-Economides, C., 2013. Permeability Estimation from Fracture Calibration Test Analysis in Shale and Tight Gas. Society of Petroleum Engineers, Denver.
Yang, Z.H., Sang, Q., Dong, M.Z., Zhang, S.J., Li, Y.J., Gong, H.J., 2015. A modified pressure-pulse decay method for determining permeabilities of tight reservoir cores. J. Nat. Gas Sci. Eng. 27, 236–246.
Zhang, D.X., Yang, T.Y., 2013. An overview of shale-gas production. Acta Pet. Sin. 34 (4), 792–801 (in Chinese).
Zhang, M., Takahashi, M., Morin, M., Esaki, T., 2000b. Evaluation and application of the transient-pulse technique for determining the hydraulic properties of low-permeability rocks-Part 2: experimental application. Geotech. Test. J. 23 (1), 91–99.
Zhang, M., Takahashi, M., Morin, R.H., Esaki, T., 2000a. Evaluation and application of the transient-pulse technique for determining the hydraulic properties of low-permeability rocks-Part 1: theoretical evaluation. Geotech. Test. J. 23 (1), 83–90.
Zhang, Y.P., Hyndman, C.L., Maini, B.B., 2000c. Measurement of gas diffusivity in heavy oils. J. Pet. Sci. Eng. 25 (1–2), 37–47.